Series Compensated PWM Inverter with Battery Supply Applied to an Isolated Induction Generator

Eduard Muljadi, *Member, IEEE,* and Thomas A. Lipo, *Fellow, IEEE*

Abstract—**This paper proposes a new series compensated induction generator / battery supply topology which provides a constant voltage and frequency at the terminals, allowing minimum current harmonic distortion while at the same time providing a source and sink of real and reactive power. With appropriate control of the reactive power, the speed of the generator is allowed to vary within a relatively wide range. This technique can be further expanded by applying ac capacitors in parallel with the load to lessen the burden of the PWM inverter. Both simulation and experimental results are in agreement with the theory which leads to the conclusion that the system could be feasible for isolated power generation systems (wind, hydro, diesel, or hybrid generation).**

I. Introduction

ALTERNATE energy sources are typically located in isolated areas where the utility supply is not available or is frequently interrupted, thereby frequently placing the energy source in isolation to supply the load. Such situations require that the alternate energy power generating system perform the voltage regulation function by providing a source not only for real power to the load but also reactive power. There are many types of excitation systems currently being employed to supply the reactive power requirements of induction generators, the most frequently used electromechanical energy converter for such applications. In particular, in an isolated system, solid-state excitation appears to be a viable candidate for the source of reactive power [1]. Despite the harmonics generated by such converter excitation, the quest for a better system solution has driven many researchers to find new means to tap the energy generated by the converter both from the ac side and from the dc side.

For wind energy systems employing an induction generator, reactive power requirements are generally supplied by switching in banks of capacitors in an attempt to roughly regulate the voltage in steps. However, the cost and complexity of such an approach has prevented widespread application of such systems. The new converter system which is proposed in this paper is intended to operate in conjunction with an isolated induction generator and utilizes a PWM inverter and battery supply for the purpose of both excitation control and energy storage. The proposed system is shown in Fig. 1 and consists of three main components: an induction machine, voltage a PWM inverter and a dc battery system. The stator winding of the induction generator is connected in series with both the three phase load and an inverter. While a simple single bridge type of PWM (pulse width modulated) inverter has been selected for the particular inverter topology, it is clear that any type of dc voltage link inverter which realizes voltage control on the ac side of the inverter could also be utilized (i.e., resonant link converters, multilevel converters, etc.). Feedback control is used to regulate the output voltage of the PWM inverter. The term PWM inverter dc battery system from hereon will be simplified to PWM-battery for simplicity.

In this system, real power is taken from the induction generator when there is sufficient input power from the prime mover or partly from the induction generator and partly from the dc battery depending on the variation of the load and input power from the prime mover. The PWM-battery functions to produce and to absorb real power or reactive power as the input mechanical power and the electrical output power changes with time. Hence, the PWM-battery acts as a buffer to ensure the balance of real and reactive power. Power distribution in the system can be manipulated to the form shown in Fig. 2 where the balance of real power is maintained by controlling the power-flow into and out of the battery. Thus, in effect, the PWM-battery combination also behaves as a sink or a source of real power [2].

The equivalent circuit of the PWM-battery system can be represented by its per phase equivalent circuit shown in Fig. 3. The PWM is represented by a fictitious variable resistance R_c (which may have a positive or negative value) and a fictitious variable reactance X_c representing equivalent capacitance needed to compensate the reactive power needed by the induction generator and the load.

Three possible conditions are represented in the phasor diagrams shown in Fig. 4.

Case I: Mechanical input power = electrical load + Losses.

Paper ICPSD 93-56, approved by the Energy Systems Committee of the IEEE Industry Applications Society for presentation at the 1993 IAS Annual Meeting. Manuscript released for publication February 21, 1994.

E. Muljadi was and T. A. Lipo is with the Department of Electrical and Computer Engineering, University of Wisconsin-Madison, 1415 Johnson Drive, Madison, WI 53706.

*E. Muljadi is currently with the National Renewable Energy Lab, Golden, Colorado.

IEEE Log Number 9402627.

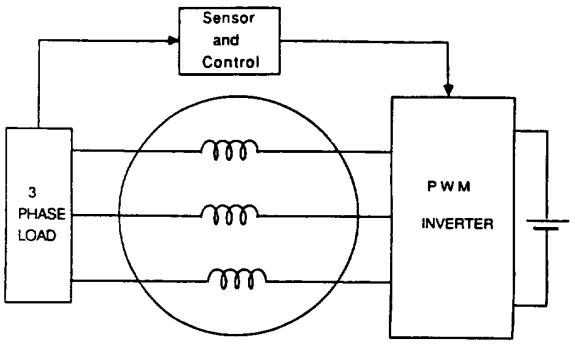

Fig. 1. Physical diagram of the system proposed.

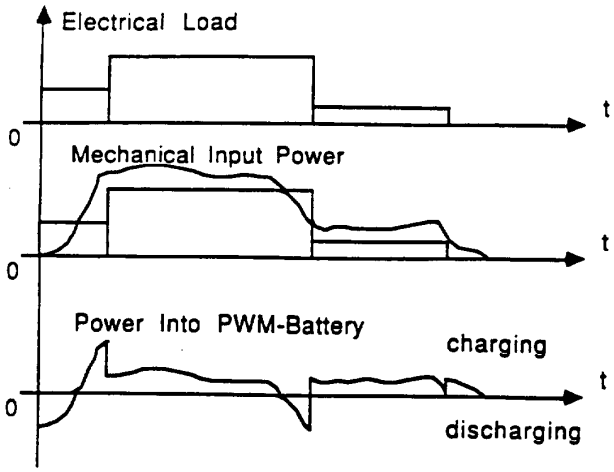

Fig. 2. Power distribution in the system.

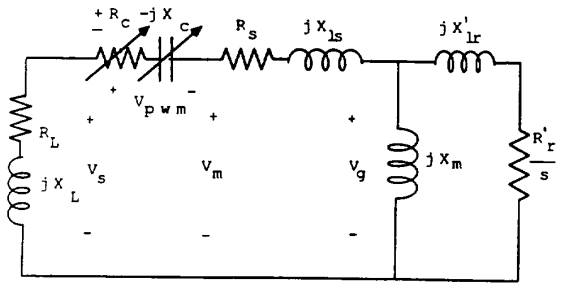

Fig. 3. Equivalent circuit for an induction generator with a series compensated PWM converter-battery combination.

Case II: Mechanical input power > electrical load + losses.

Case III: Mechanical input power < electrical load + losses.

Case I represents a condition where the PWM-battery acts as a source and sink of reactive power. There is no interchange of real power between the PWM-battery and the induction generator. Case II represents a condition

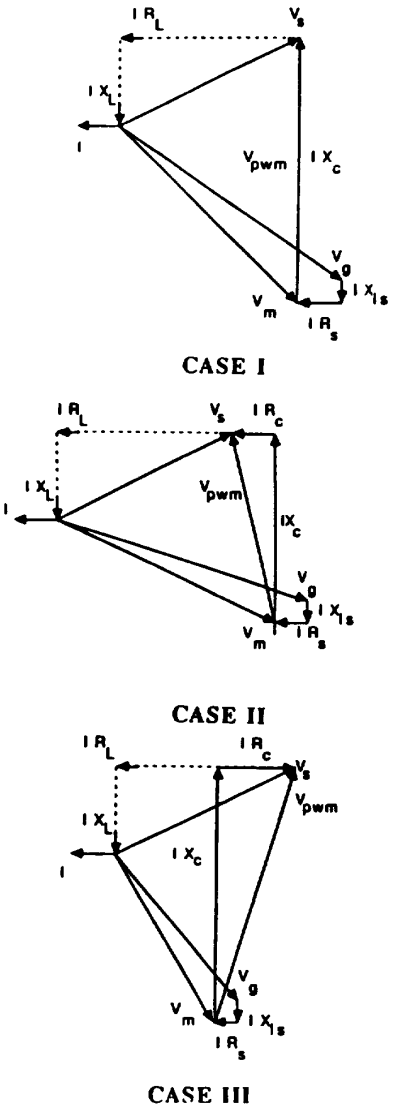

Fig. 4. Phasor diagram for real and reactive power interchange in the series compensated PWM-battery.

where the PWM-battery absorbs real power. The incoming energy is stored in the battery and the battery is charged. Case III represents a condition where there is not enough power generated by the induction generator. Thus the PWM-battery supplies real power to the load. The battery is discharged to cover the power needed by the load.

In the next section, series compensation using a PWM-battery supply if discussed along with the equations needed to accommodate these three operating conditions. Saturation of the magnetic field is included in a digital computer program as well with an analog computer. The analog computer was also used to study the dynamics and the wave-form of the voltages and the current.

II. PWM-Battery Compensation

The dc-battery portion of the system can be viewed as a buffer to compensate for the fluctuation of real power generated from the mechanical input prime mover. The rating of the induction generator must be capable of absorbing the maximum allowable input power from the prime mover. The PWM-battery can also be assumed to be a buffer of reactive power [2], since the dc battery in effect functions as a very large dc capacitor. From the equivalent circuit point of view, the PWM-battery can be viewed as an active impedance whose size and polarity correspond to the power flow in the PWM converter.

The PWM-Battery is represented by a resistor R_c and capacitor X_c. The sign of the R_c can be positive when the battery is absorbing real power from the system, or negative when the battery is supplying real power into the system. The sign of X_c is negative, assuming that the load connected to the generator (in most cases) is an inductive load. The voltage across the load can be maintained as constant by adjusting the active impedance of the PWM-battery. If at constant load, i.e., constant R_L, X_L, the voltage across the load is to be maintained constant, the current through the load must also be kept constant. This constraint makes the system behave as a current source so that the PWM-battery should be controlled in a manner similar to that with a current source inverter. To solve the equations for the induction generator mode, the following equations must be satisfied

$$\bar{I} = \frac{\bar{V}_s}{(R_L + jX_L)}, \tag{1}$$

where V_S is the rms terminal voltage, I is the rms stator or load current, and R_L, X_L is the load connected at the output terminals

Since the current around the series loop is the same, the following equation must be valid

$$\frac{\bar{V}_g}{\bar{Z}_g} = \frac{\bar{V}_s}{(R_L + jX_L)} \tag{2}$$

or since only the magnitude is important, this expression can be rewritten as

$$\left|\frac{V_g}{Z_g}\right|^2 = \left|\frac{V_s}{(R_L + jX_L)}\right|^2, \tag{3}$$

which can be simplified to

$$|Z_g|^2 = A, \tag{4}$$

where

$$A = \frac{(R_L^2 + X_L^2)}{\left[\frac{V_s}{V_g}\right]^2}.$$

Upon solving, the above equation can be written in simplified form as

$$\bar{Z}_g = R_g + jX_g = jX_m \left\| \left(\frac{R'_r}{S} + jX'_{1r}\right),\right.$$

or,

$$a_2 S_r^4 + a_1 S_r^2 + a_0 = 0, \tag{5}$$

where

$$a_2 = X_{1r}'^2 X_r'^2 X_m^2 - A X_r'^4,$$
$$a_1 = \left(X_m^4 + 2X'_{1r} X'_r X_m^2 - 2A X_r'^2\right),$$
$$a_0 = X_m^2 - A,$$
$$S_r = \frac{S}{R'_r}.$$

Only one value of negative slip in the operating region is useful for the generating mode. Given the terminal voltage V_S, the parameters of the induction machine and the load R_L, X_L the slip can be solved for each pair of V_g, X_m. The equation for the electrical torque can be written as follows

$$T = kI^2 R_g \tag{6}$$

$$= k\frac{V_s^2}{(R_L^2 + X_L^2)} \frac{\left(\frac{R'_r}{S} X_m^2\right)}{\left(\frac{R_r'^2}{S} + X_r'^2\right)}, \tag{7}$$

where

$$X'_r = X_m + X'_{1r},$$
$$k = \frac{3}{\omega_s}\frac{\text{poles}}{2}.$$

The maximum value of torque $T_{\max}$ occurs at

$$S_{\max} = \pm \frac{R'_r}{X'_r} \tag{8}$$

and the maximum torque is

$$T_{\max} = k\frac{V_s^2}{(R_L^2 + X_L^2)} \frac{X_m^2}{2X'_r}. \tag{9}$$

III. Admittance Dagram Approach

The concept of the admittance diagram can be applied to analyze the PWM-battery concept. The advantage of the PWM-battery is its flexibility in sizing the equivalent resistance and reactance in series with the induction generator. The interesting characteristic of the PWM-battery combination is the capability of expanding or reducing the radius of the stator-load admittance circle in the admittance diagram. In general, the total admittance in the diagram must satisfy the conservation of real and reactive power whereby the total admittance is equal to zero at any condition. Hence, the real part of the total admittance is zero and the imaginary of the total admittance part is also zero. The sum of the rotor and magnetizing

admittance must be compensated by the stator/load (including the PWM-battery) admittance. By utilizing the PWM-battery the admittance can be made to follow the new condition by regulating the radius of the stator/load admittance circle ($\pm R_c$) and the size of X_c.

From the equivalent circuit, the admittance diagram can be simplified to the following equations. In particular, the stator, PWM-battery and the load admittance can be written as:

$$\overline{Z_1} = (R_s + R_L \pm R_c) + j(X_{1s} + X_L \pm X_c) = R_1 + jX_1. \quad (10)$$

The impedance can be expressed in terms of its admittance as

$$\overline{Z}_1 = \frac{1}{\overline{Y_1}} = \frac{G_1}{G_1^2 + B_1^2} + j\frac{B_1}{G_1^2 + B_1^2}. \quad (11)$$

The real part of the impedance can be rearranged as follow

$$\left(G_1 - \frac{1}{2R_1}\right)^2 + B_1^2 = \frac{1}{(2R_1)^2}. \quad (12)$$

Thus, the equation to describe the stator circuit of the induction generator can be expressed as the locus of a circle with a radius of $1/(2R_1)$ where R_1 is the real part of the impedance of the stator, the load and the PWM-battery. The size of the radius, for a constant resistive load, is adjustable by regulating the real power into and out of the PWM-battery. As the size of the imaginary part of the impedance (X_1) is varied, the operating points travels along the perimeter of the circle. The size of X_1 can be changed by varying the fictitious X_c of the PWM-battery (by generating more reactive power). The stator-load-PWM admittance is represented by a phasor starting from the origin to the point on the perimeter of the semi-circle. The size of the current is proportional to the size of the stator admittance multiplied by the air-gap voltage. Similarly the radius of the semicircle can be controlled by adjusting the fictitious resistance R_c which is essentially adjusting the real-power flow in and out of the PWM-battery.

It should be noted that the size of the magnetizing branch inductance varies with the saturation level. During high saturation the size of the inductance becomes lower than the size at rated condition. The rotor branch can be represented as an equation of a circle with the radius proportional to $(1/2X'_{lr})$ where X'_{lr} is the leakage reactance of the rotor circuit. As the slip varies the operating point travels along the perimeter of the circle. The admittance of the rotor branch is represented by a phasor starting from the crossing point between the vertical axis and the semicircle to the point on the perimeter of the circle.

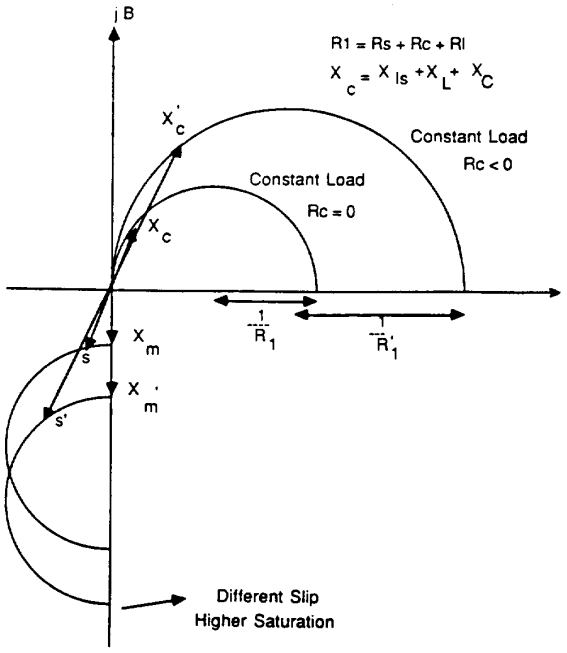

Fig. 5. Admittance diagram for a series compensated PWM-battery.

$$\overline{Z'_r} = \frac{R'_r}{S} + jX'_{lr}, \quad (13)$$

$$\overline{Y'_r} = G_2 + jB_2, \quad (14)$$

$$G_2^2 + \left(B_2 + \frac{1}{2X'_{lr}}\right)^2 = \frac{1}{(2X'_{lr})^2}. \quad (15)$$

Conservation of real and reactive power is maintained by balancing the admittance of the rotor and magnetizing branch with the admittance of the stator-load-PWM. This can be accomplished due to the fact that the PWM-battery has and adjustable value of R_c and X_c. The complete representation of the admittance diagram is shown in Fig. 5.

IV. Steady-State Analysis

Since the system under investigation behaves as a current source, the torque at a particular slip depends only on the size of the current and is proportional to the square of the stator current (if saturation is neglected). The type of load does not affect the torque versus slip curve. Fig. 6(a) shows the torque curves versus slip for a resistive load. It can be seen that the slip for the peak torque changes with saturation. Operation in the smaller slip region results in a heavier saturation region. As the load becomes larger, the current becomes larger and the slip at maximum torque also moves to a larger slip (more negative). This observation is consistent with the equation for the slip at maximum torque. Fig. 6(b) shows the case of a constant impedance with a variable power factor. In this case, since the size of the impedance and terminal

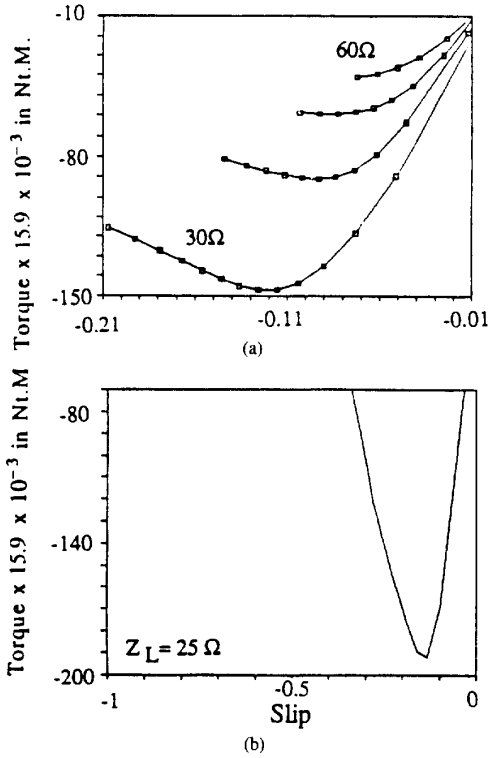

Fig. 6. Torque versus slip at various load (V_s = 50 volts): (a) Z_L = $30\angle 0^0$ to $60\angle 0^0$ ohms and (b) Z_L = $25\angle 0^0$ to $60\angle 90^0$ ohms.

voltage are kept constant, the torque size is also the same, regardless of the power factor of the induction machine.

It is clear that the demand from PWM inverter depends upon the balance between power input and power output. If the mechanical input power is greater than the electrical output power, the excess energy will be stored in the battery. On the other hand if the mechanical input power is smaller than the electrical output power, the power shortage will be taken from the PWM-battery.

Fig. 7 shows the relationship between the PWM power and the slip for resistive load at a constant terminal voltage. It is indicated that the load size has a significant effect on the real power interchange in the PWM-battery.

The real and reactive power flow in the PWM-battery can be represented by the equivalent impedance $R_c + jX_c$ whose real part depend upon the size and direction of power flow. For each load, the R_c curves have the same shape as the corresponding real power output of the PWM and the X_c curves have the same shape as the reactive power output of the PWM. In Fig. 8(a) is shown the shape of the resistive impedance of the PWM with respect to the slip for different loads. It can be seen that the shapes of the curves are similar to that for the power output of the PWM except that the scale depends on the load current. The crossing points of the curves with the horizontal axis (slip) are those slips at which the PWM-battery does not supply real power but functions instead as a PWM = dc capacitor which provides only reactive

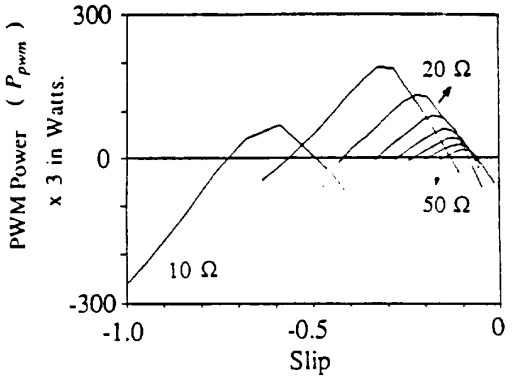

Fig. 7. PWM power versus slip at V_s = 50 volts: Z_L = $10\angle 0^0$ to $50\angle 0^0$ ohms.

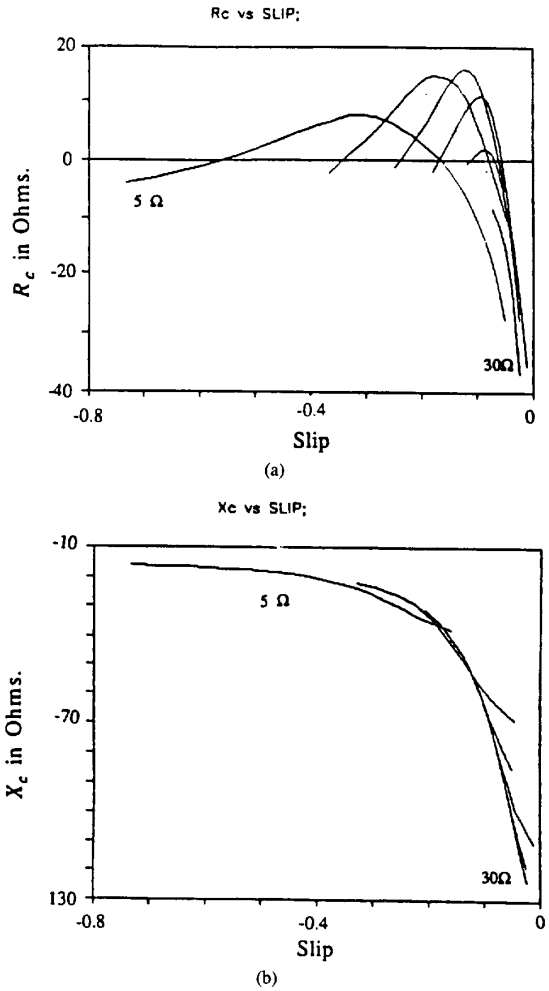

Fig. 8. Equivalent impedance for a PWM-battery: (a) R_c with Z_L = $5\angle 0^0$ to $30\angle 0^0$ ohms and (b) X_c with Z_L = $5\angle 0^0$ to $30\angle 0^0$ ohms.

power. The reactance X_c versus slip for different loads, indicating the reactive power contribution of the PWM-battery is shown in Fig. 8(b). Note that there is no crossing point with the slip axis, which means that there is always a need for reactive power to magnetize the induction machine regardless of the slip.

V. Analog Computer Simulation

The previous discussions have been based on steady state calculation done in a digital computer. Only the fundamental component of the PWM output was considered and the PWM-battery was treated as an equivalent variable impedance. In order to obtain a better understanding of the PWM-battery compensation, a simulation was also perform using an analog computer. This approach gives more realistic results from the point of view of stability, and improved current and voltages waveforms.

The saturation effect can be simulated in the analog computer by using the method suggested by He and Lipo [3], [4] for synchronously rotating frame or by using the method suggested by Lipo and Consoli [5] for the stationary reference frame. The latter has been used in this work, since this method is easy implemented and gives a satisfactory result for simulating the induction generator.

Work on the analog computer was specifically directed to the study of a PWM-battery series compensation scheme with a resistive load. The slip was adjusted from a low slip to a high slip condition. Observations included various terminal voltage settings and effects on the other variables. The induction machine simulated was a specially designed three phase inducation machine of 172, 270 volts/phase. The parameters of the induction machine are given in the appendix. The analog circuit diagram for induction machine and other circuit is also given in the appendix.

Fig. 9 shows the traces for a continuous slip variation. The trace of load current shows that the current is constant when the slip varies while maintaining constant terminal voltage, while the PWM voltage changes from a higher voltage at low power factor (small slip) to a smaller voltage as the power factor increases.

The power factor clearly has a very significant effect on the size of the PWM output voltage. The torque also changes with the slip and reaches a maximum at a particular value of slip. The dc current of the PWM follows the nature of the real power interchange between the real power produced by the induction machine and the real power consumed by the load and losses in the machine. The real power produced by the PWM is directly proportional to the dc current since the voltage across the battery must be designed to be approximately constant due to the fact that over-discharging the battery could lead to a failure of the battery. The reactive power produced by the PWM is always positive since the induction machine operates at a lagging power factor. Minimum reactive power occurs at a maximum power factor which occur at the same instance as the minimum output voltage of the PWM.

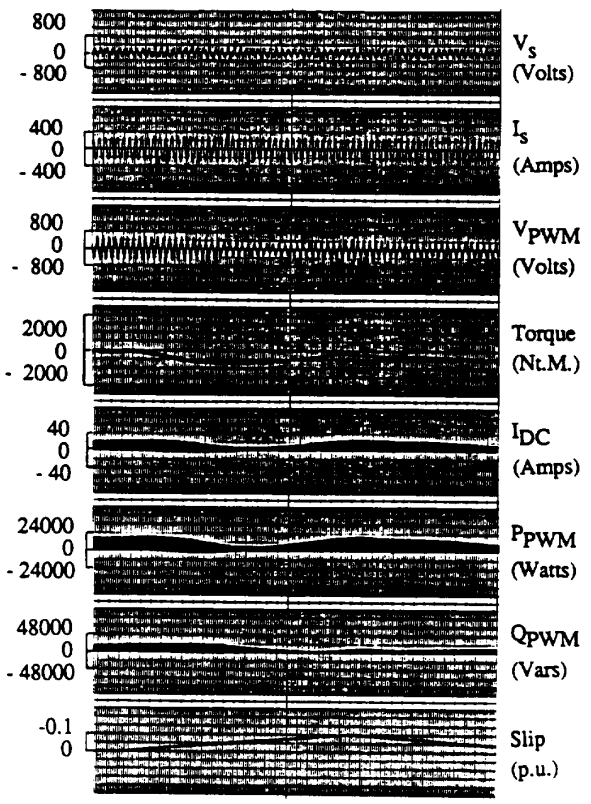

Fig. 9. Analog traces for V_s = 170 volts (rms) at rated current with slip = 0 to -0.1 and $Z_L = 0.85 \angle 0^0$ ohms.

Fig. 10 presents the results for three different slip operating conditions. The expanded waveforms are also shown. It is apparent that for resistive loads both the voltage and the current wave forms are smooth because all the harmonics distortion produced by the PWM is filtered by the induction machine winding.

For lower slip regions, the output voltage of the PWM must be modulated in such a manner so as to produce a higher voltage since this slip is related to the low power factor condition (refer to the phasor diagram). The dc current and the real power produced by the PWM is positive which means that the battery is discharging. As the slip is increased the power factor is improved and there is less real power produced by the PWM since the inducation machine begins to produce more real power. The reactive power produced by the PWM is also reduced as the power factor is improved. However, as the slip is further increased, more losses are produced as a result of losses in the rotor. The real power produced by the PWM must therefore again be increased.

VI. Experimental Results

An experimental study was also carried out in this study. The laboratory portion of this work used a three phase induction machine, a series connected PWM inverter and an adjustable R_L load. To avoid any possibility

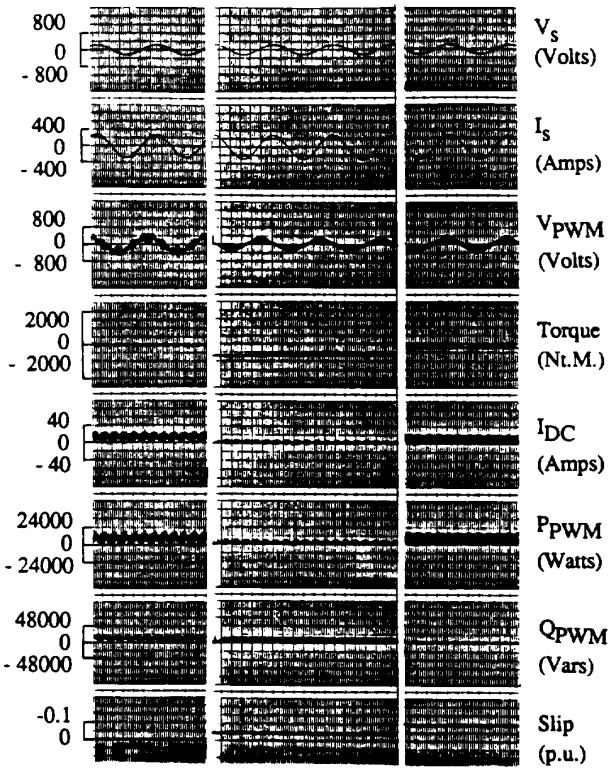

Fig. 10. Analog traces for V_s = 170 volts (rms) at rated current and $Z_L = 0.85\angle 0^0$ ohms at (a) slip = 0; (b) slip = −0.05; (c) slip = −0.1.

of ground faults, the system was totally isolated from ground by using isolation transformers. The end terminals of the stator winding was designed to be connected in a star connection. However, one set of end windings was connected to a balanced three phase load, and the other set of end windings (after the star connection was opened) was connected to the PWM-battery. The ratings of the induction machine are 1/3 hp with 1.4 amps rated current and rated voltage of 220 volts.

The experiment was performed by loading the induction generator with different types of loads (sizes and power factors). The dc bus voltage was maintained at 280 volts dc. The carrier frequency of the PWM modulation was set to 2.4 kHz. The speed of the generator was varied from 1800 rpm to 2400 rpm (slip = 0.0 to slip = −0.3333) and the output frequency was set constant at 60 hz.

A. dc Battery Power vs Slip

In these tests, the power measured was the dc power (entering the battery) as an indicator of the power that can be absorbed or generated by the dc bus (battery). It is clear that the dc power interchange between the battery and the system depends upon the mechanical input power and the electrical output power taken from the terminal output of the generator. The more power taken out of the terminal output of the generator, the less power that can be stored in the battery. Therefore, in the application of

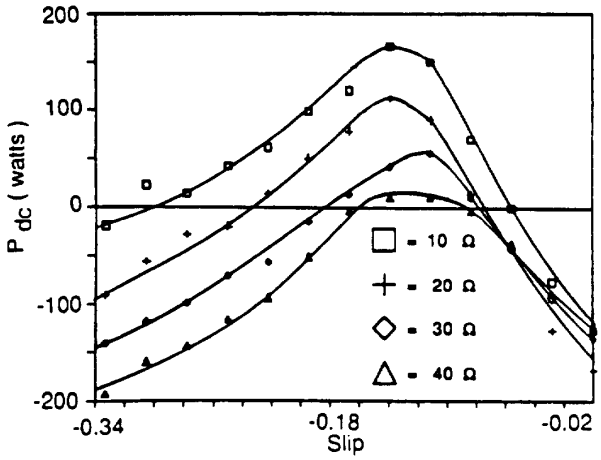

Fig. 11. dc Power versus slip (experimental data) at load current I_s = 1.4 amps (rms).

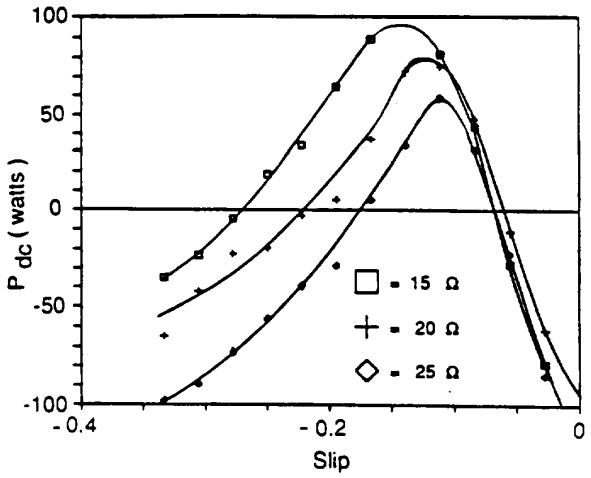

Fig. 12. dc Power versus slip (experimental data) at V_s = 28 volts (rms).

the system, the operating region of the electrical load, speed and the mechanical aspects of design must be carefully considered.

In the experimental results shown in Fig. 11, the resistive load applied ranges from 20 Ω to 40 Ω and for each load the speed of the generator was varied from 1800 rpm to 2400 rpm. The currents were maintained at 1.4 amps (rated current). It is apparent that lower resistor load generates more power into the dc bus at the same slip when compared to a larger resistive load. This fact is explained by considering that at constant output current (i.e., 1.4 amps in this case) the mechanical input power (torque) is the same, while the power absorbed by the load is proportional to the resistor size. Therefore the net output of the generator is used to supply the load demand and losses and the excess is used to charge the dc battery.

B. Resistive Load with Constant Terminal Voltage

In this case the resistive load was set to 15, 20, and 25 Ω while maintaining a constant terminal voltage. For each

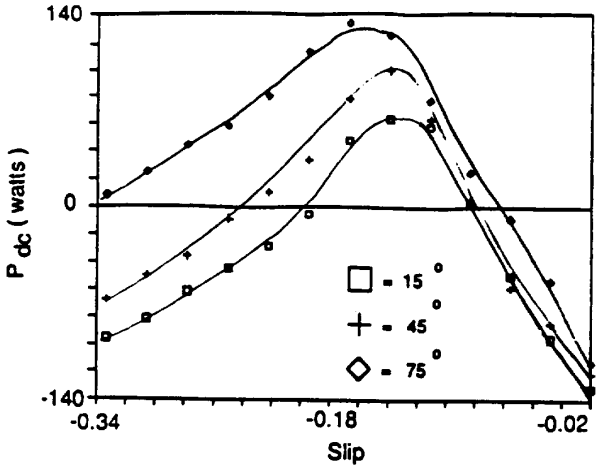

Fig. 13. dc Power versus slip (experimental data) at V_s = 28 volts (rms) and Z_{load} = 20 ohms with power factor varied.

resistive load, the speed of the generator was varied from 1800 to 2400 rpm. The voltage across the load was maintained constant (28 volts). Therefore, the load currents varied from 1.87 amps for a resistive load of 15 Ω to 1.12 amps at 25 Ω load. Saturation can be expected to be the highest at current of 1.87 amps, especially at a small slip. By comparing the results for three different loads, as shown in Fig. 12, it can be determined that the largest power that can be stored in the battery is for the load of 15 Ω. This observation is also apparent from a conceptual point of view since for 15 Ω load, the load current is also larger, which means that the torque and mechanical input power is higher, although the load consumption is larger due to the higher current.

C. Constant Impedance at Different Power Factor

In this test the load impedance was set to 20 Ω and the power factor was varied from 0.26 to 0.97 while the terminal voltage was fixed as a constant. For each load, the speed was varied from 1800 to 2400 rpm. Since the voltage across the load was maintained to be constant (28 volts), the current was also constant at 1.4 amps. Although the current through and the voltage across the load is constant, the power consumed by the load, is not equal to different power factors. Since the current in the system is the same, the torque and mechanical input power are also the same. Therefore, at a lower power factor more power can be stored in the dc battery (refer to Fig. 13).

D. Voltage and Current Waveforms

In this proposed system a PWM inverter is used to maintain the system frequency constant and to supply the reactive power required both for the load and the induction machine. Although the converter inherently generates harmonics as well as the desired fundamental component, the series connection of the system utilizes the inductance of the induction machine as the filter to these harmonics. An illustration of this filtering effect is shown in Fig. 14 for a resistive load. In particular, the voltage across the induction machine winding is shown for two different speeds. It can be noted that the voltage output across the terminal of the induction generator is very smooth.

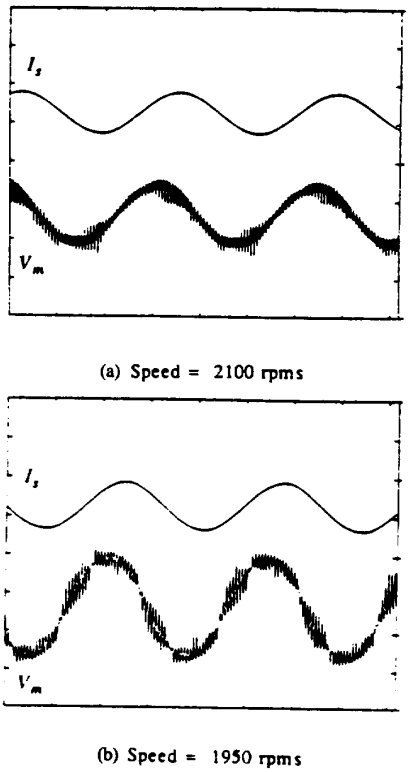

Fig. 14. Voltage across phase winding and current at V_s = 20 volts (rms); R_{load} = 14.4 ohms; X_{load} = 14.4 ohms; voltage scale = 125 V/div, current scale = 2.5 A/div; time scale = 50 ms/div.

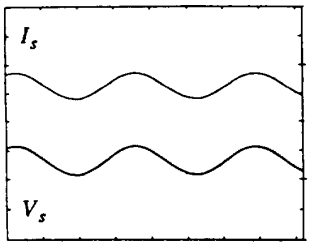

(a) Speed = 2100 rpms

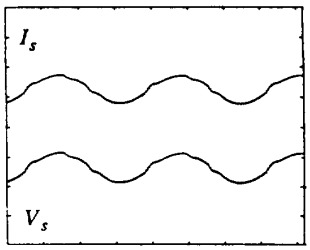

(b) Speed = 2000 rpms

Fig. 15. Terminal Voltage and Current for a resistive load at V_s = 17.5 volts (rms); R_{load} = 20 ohms; voltage scale = 50 V/div; current scale = 2.5 A/div; time scale = 50 ms/div.

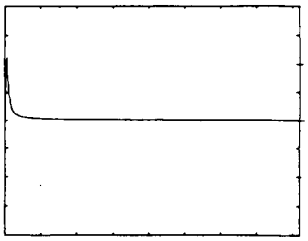

(a) Speed = 2100 rpms

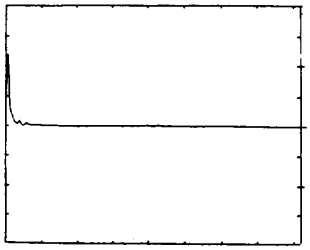

(b) Speed = 2000 rpms

Fig. 16. Frequency spectrum of the terminal voltage for the resistive load R_{load} = 20 ohms at voltage = 17.5 volts, voltage scale = 7.25 V/div; frequency scale = 652 Hz/div; time scale = 50 ms/div.

It is also useful to examine Fig. 15 where a resistive load is again applied to the induction generator. The speed of the induction generator was varied in this case. For the speed set at 2100 rpm [Fig. 15(a)], the power factor of the induction machine was high, the PWM output voltage was low since the induction machine did not require considerable reactive power or excitation. The waveform is very sinusoidal. As the speed of the induction generator was lowered (by lowering the slip), the power factor of the induction machine was also lower. At the speed of 2000 rpm [Fig. 15(b)] the PWM converter had to be modulated higher and the output waveform of the PWM inverter was closer to a quasi square wave form. As a result the output waveform contains of more fifth and seventh harmonics. At even lower speed (at 1900 rpm), the power factor of the induction machine was lower and the PWM output voltage became a quasi square wave. As can be noted the output waveform becomes considerably distorted.

To quantify the harmonic distortion observed in these tests, the frequency spectrum of the voltage waveforms at different speeds are presented in the charts shown in Fig. 16. It can be seen very clearly that the magnitude of the fundamental component is the largest while the higher harmonics components vary widely with the speed. Clearly, harmonic limits need to be defined to fix the allowable speed range of the induction generator.

VII. Conclusion

Most systems employing induction generators are connected to the grid and the control of voltage amplitude and frequency is simply provided by the grid. However, isolated generating system impose special problems on system design. For example, it is necessary to ensure maintenance of constant frequency and voltage over varying rotor speeds. Also it is necessary to minimize the harmonic distortion resulting from inverter excitation. Finally, it is necessary to provide a source and sink for the real power. In this paper a new system has been proposed that compensates for all of the above deficiencies encountered in isolated generating systems. This system consists of three major elements:

- an induction generator to generate electric power and to filter the current harmonics,
- a PWM inverter to provide the excitation and set the desired frequency,
- an energy storage dc battery to allow a bidirectional power flow.

An investigation into the ideal sinusoidal steady state as well as a detailed simulation of the overall system has been conducted. It has been demonstrated that the results agree well with the experimental data. This new concept should find use in a variety of applications involving prime movers which operate best over a variable speed including isolated wind turbines, variable head hydro and other similar situations.

Acknowledgment

This work reported in this paper was carried out at the University of Wisconsin Madison. The authors wish to thank the Wisconsin Electric Machines and Power Electronic Consortium (WEMPEC) for sponsoring this project. The authors also wish to thank the National Renewable Energy Lab (NREL) for the support provided.

APPENDIX

Induction Machine Data for Digital Computation and Laboratory Experiment

Nameplate Data :	
Wagner-Leland	3 Phase
208-220 Volts	1.4 Amps
1725 RPM	60 Hz
Parameter Values :	
r_s = 7.4 ohms	r_r' = 11.25 ohms
X_{ls} = 7.4 ohms	X_{lr}' = 7.45 ohms
X_m' = 116.16 ohms	(rated)

Induction Machine Data for Analog Simulation :

Nameplate Data :	
172 HP	3 Phase
468 Volts	180 Amps
1200 RPM	43 Hz
Parameter Values :	
r_s = 0.0217 ohms	r_r' = 0.0329 ohms
X_{ls} = 0.0874 ohms	X_{lr}' = 0.0996 ohms
X_m' = 3.6493 ohms	J = 11.4 kg-m^2

REFERENCES

[1] P. K. Sood, H. Rehaoulia, D. W. Novotny, and T. A. Lipo, "A pulse width controlled three switch exciter for induction machines," *IEEE IAS Annual Meeting*, pp. 653–661, Oct. 6–11, 1985.

[2] E. Muljadi, "Series compensated PWM inverter with battery supply applied to an isolated operation of induction generator," Ph.D. thesis, Univ. of Wisconsin, Madison, 1987.

[3] Y. K. He and T. A. Lipo, "Computer simulation of an induction machine with spatially dependent saturation," *IEEE Trans. Power App. Syst.*, vol. PAS-103, no. 4, pp. 707–714, April 1984.

[4] Y. K. He and T. A. Lipo, "Saturation effects in the stability analysis of a VSI induction motor drive," *Trans. Elect. Engineers (Japan)*, vol. 103, no. 11/12, pp. 117–124, Nov./Dec. 1983.

[5] T. A. Lipo and A. Consoli, "Modelling and simulation of induction motors with saturable leakage reactances," *IEEE Trans. Ind. Appl.*, vol. IA-20, Jan./Feb. 1984, pp. 180–189.

Eduard Muljadi (M'82) received his B.S.E.E. degree from Surabaya Institute of Technology, in 1981, M.S., and Ph.D. degrees from the University of Wisconsin, Madison in 1984 and 1987, respectively.

He was an associate professor at the Department of Electrical and Computer Engineering at the California State University, Fresno, before he joined National Renewable Energy Laboratory, Golden, Colorado in June 1992. His research interests are in the fields of power systems, electric machines, and power electronics with applications in wind power generation. He is member of IEEE, SME, Sigma Xi, and Eta Kappa Nu.

Thomas A. Lipo (M'64-SM'71-F'87) is a native of Milwaukee Wisconsin. He received his B.E.E. and M.S.E.E. degrees from Marquette University, Milwaukee, WI in 1962 and 1964 and the Ph.D. degree in electrical engineering from the University of Wisconsin in 1968. From 1969 to 1979 he was an Electrical Engineer in the Power Electronics Laboratory of Corporate Research and Development of the General Electric Company, Schenectady, NY. He became Professor of Electrical Engineering at Purdue University in 1979 and in 1981 he joined the University of Wisconsin in the same capacity where he is presently the W. W. Grainger Professor for Power Electronics and Electrical Machines.

Dr. Lipo has been engaged in power electronics research for over 30 years. He has received eleven patents and has 15 IEEE prize paper awards for his work including co-recipient of the Best Paper Award in the IEEE Industry Applications Society Transactions for the year 1984. In 1986 he received the Outstanding Achievement Award from the IEEE Industry Applications Society for his contributions to the field of ac drives and in 1990 he received the William E. Newell Award of the IEEE Power Electronics Society for contributions to field of power electronics. He is the President of the IAS during 1994.